

Structural Evaluation of Phospholipid Bicelles for Solution-State Studies of Membrane-Associated Biomolecules

Kerney J. Glover,* Jennifer A. Whiles,* Guohua Wu,[†] Nan-jun Yu,[‡] Raymond Deems,* Jochem O. Struppe,* Ruth E. Stark,[†] Elizabeth A. Komives,* and Regitze R. Vold*

*Department of Chemistry and Biochemistry, University of California, San Diego, La Jolla, California 92093-0359 USA; [†]Department of Chemistry, City University of New York Graduate Center and College of Staten Island, Staten Island, New York 10314-6600 USA; and [‡]Department of Chemistry and Biochemistry, University of California, Los Angeles, Los Angeles, California 90024 USA

ABSTRACT Several complementary physical techniques have been used to characterize the aggregate structures formed in solutions containing dimyristoylphosphatidylcholine (DMPC)/dihexanoylphosphatidylcholine (DHPC) at ratios of ≤ 0.5 and to establish their morphology and lipid organization as that of bicelles. ³¹P NMR studies showed that the DMPC and DHPC components were highly segregated over a wide range of DMPC/DHPC ratios ($q = 0.05$ – 0.5) and temperatures (15°C and 37°C). Only at phospholipid concentrations below 130 mM did the bicelles appear to undergo a change in morphology. These results were corroborated by fluorescence data, which demonstrated the inverse dependence of bicelle size on phospholipid concentration as well as a distinctive change in phospholipid arrangement at low concentrations. In addition, dynamic light scattering and electron microscopy studies supported the hypothesis that the bicellar phospholipid aggregates are disk-shaped. The radius of the planar domain of the disk was found to be directly proportional to the ratio of DMPC/DHPC and inversely proportional to the total phospholipid concentration when the DMPC/DHPC ratio was held constant at 0.5. Taken together, these results suggest that bicelles with low q retain the morphology and bilayer organization typical of their liquid-crystalline counterparts, making them useful membrane mimetics.

INTRODUCTION

Bicelles have emerged as a powerful medium for studying membrane-associated biomolecules. A bicelle is a discoidal lipid aggregate composed of long-chain phospholipid and detergent. Previous studies of lipid aggregates have suggested that the morphology may depend on the total phospholipid concentration, the ratio of the constituents, and the temperature (Gabriel and Roberts, 1984; Sanders et al., 1994). The distinguishing structural feature of a bicelle is a central planar bilayer formed by the long-chain phospholipid surrounded by a rim of detergent that shields the long-chain lipid tails from water (Fig. 1) (Ram and Prestegard, 1988; Sanders et al., 1994; Vold and Prosser, 1996). The planar region is most commonly composed of dimyristoylphosphatidylcholine (DMPC), which may be doped with phospholipids that have identical chain lengths but different headgroups (e.g., dimyristoylphosphatidylserine or dimyristoylphosphatidylglycerol) to alter the charge characteristics of the membrane (Struppe et al., 2000). The rim, on the other hand, may be composed of either a bile-salt derivative such as 3-(cholamidopropyl)dimethylammonio-2-hydroxy-1-propane-sulfonate (CHAPSO) or a short-chain phospholipid such as dihexanoylphosphatidylcholine

(DHPC) (Sanders and Prestegard, 1990; Sanders and Schwonek, 1992; Sanders et al., 1993).

Spontaneous alignment in magnetic fields of >2 T has been reported for bicelles with $2.5 < q < 5$ and $c_L \approx$

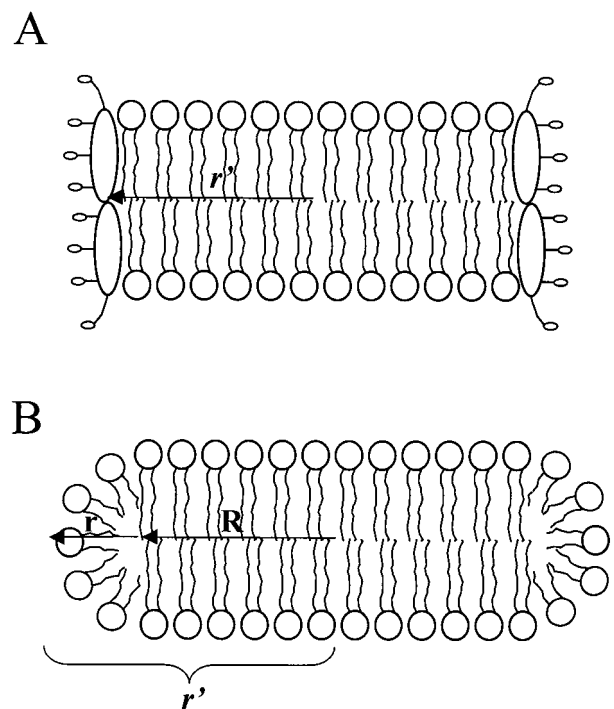


FIGURE 1 Schematic representation of DMPC bicelles with a CHAPSO rim (A) and a DHPC rim (B). A more refined model of bile salt-phosphatidylcholine mixed micelles includes additional bile salt molecules that interact hydrophobically with the PC acyl chains (Cohen et al., 1998). The designated particle radii are described in the text.

Received for publication 6 February 2001 and in final form 27 June 2001.

K.J.G. and J.A.W. contributed equally to this work.

R.R.V. is deceased.

Address reprint requests to Dr. Elizabeth A. Komives, University of California, San Diego, 9500 Gilman Drive, La Jolla, CA 92093-0359. Tel.: 858-534-3058; Fax: 858-534-6174; E-mail: ekomives@ucsd.edu.

© 2001 by the Biophysical Society

0006-3495/01/10/2163/09 \$2.00

15–25% (w/w), where q is the molar ratio of DMPC to DHPC and c_L is the total phospholipid concentration. This property has made it possible to examine peptide and lipid order using solid-state NMR techniques (Howard and Opella, 1996; Losonczi and Prestegard, 1998b; Sanders et al., 1994; Sanders and Landis, 1995; Sanders and Prestegard, 1990; Struppe et al., 1998; Whiles et al., 2001). Dilute bicellar solutions ($q > 2$ and $c_L \approx 3$ –5% (w/w)) have been used to achieve a small degree of orientation of non-membrane-associated biomolecules for the purpose of obtaining residual dipolar couplings used in the refinement of high-resolution NMR structures (Tjandra and Bax, 1997; Struppe and Vold, 1998).

Using a bicelle structural model in which q controls bicelle size and c_L controls the number of aggregates, we have expanded the versatility of bicelles with the introduction of smaller bicelles ($q = 0.5$, $c_L \approx 15\%$ (w/w)) that do not align in the magnetic field. These bicelles have been shown to be suitable for high-resolution solution-state NMR studies of the structure and dynamics of membrane-associated peptides (Vold et al., 1997; Whiles et al., 2001). However, the exact morphology of these isotropic bicelles has yet to be fully characterized. In this work, we have used ^{31}P NMR, fluorescence, dynamic light scattering, and electron microscopy techniques to demonstrate that isotropic bicelles are indeed simply smaller versions of their alignable counterparts, that their discoidal shape and lipid segregation are maintained over a wide range of lipid concentrations, and that they likely contain the bilayer organization that is desirable in a mimetic membrane. Furthermore, the results of our physical measurements fit well with the predictions made for ideal bicelle structures and with ^1H -NMR and neutron scattering data being reported by Prosser's group (Vold and Prosser, 1996; S. Prosser, unpublished results).

MATERIALS AND METHODS

Materials

DMPC and DHPC were obtained from Avanti Polar Lipids (Alabaster, AL) and used without further purification. Deuterium oxide was obtained from Cambridge Isotope Labs (Andover, MA). Praseodymium(III) chloride hexahydrate (99.9%) was purchased from Aldrich Chemical Co. (Milwaukee, WI), and 8-aminophthalene-1,3,6-trisulfonic acid disodium salt (ANTS) was purchased from Molecular Probes (Eugene, OR).

^{31}P NMR

A 25% (w/w) stock bicelle solution ($q = 0.5$) was prepared by suspending the appropriate amount of DMPC in H_2O . The samples were vortexed and briefly centrifuged (at low speed and room temperature), and the pellets were resuspended with vortexing. Repeating this cycle two to three times resulted in uniform dispersions of DMPC. DHPC from a stock solution (25% (w/w) in water) was added to the DMPC dispersion to achieve $q = 0.5$. The samples were vortexed and centrifuged until they were clear and homogeneous. No pelleted lipid was separated from the sample after each

centrifugation step; instead, it was resuspended on the next cycle of vortexing and heated briefly until no pellet formed upon further centrifugation. Samples with $q = 0.5$ and various c_L values were prepared by addition of the appropriate amounts of the 25% (w/w) stock bicelle solution, D_2O , and 3 M acetate buffer (pH 5.6). Samples were diluted to a final volume of 500 μl , yielding final concentrations of 10% D_2O and 20 mM acetate. Selected samples contained PrCl_3 that was added to yield a final concentration of 197 mM (a Pr^{3+} :phospholipid ratio sufficient to saturate the lanthanide-phospholipid interaction (Kumar and Baumann, 1991)).

All spectra were recorded on a Bruker DRX600 spectrometer equipped with either a 5-mm BBI or TXI probe. One-dimensional ^{31}P spectra were recorded at 15°C or 37°C using a proton-decoupled single-pulse experiment with 32–13,561 scans for $c_L = 252$ mM to 3 mM. All spectra were recorded with 16,384 complex points and a sweep width of 100 ppm. The carrier frequency was set to 0 ppm for samples without lanthanide and to 50 ppm for samples containing lanthanide salts. All experiments were processed with the MSI Felix 97.0 software package (San Diego, CA). After Fourier transformation, the spectra were referenced to the carrier frequency to make comparisons of peak positions within each data set (i.e., with varying c_L).

Fluorescence spectroscopy

Bicelle samples were prepared as for ^{31}P NMR (from a 25% bicelle stock solution), with an appropriate amount of ANTS added from a stock solution. The final solutions contained 5 μM ANTS and 20 mM acetate, pH 5.6. Spectra were obtained at 15°C and 37°C on a Perkin-Elmer LB50B luminescence spectrometer. The excitation wavelength was 360 nm.

Dynamic light scattering

Bicelles for laser light scattering (QLS) were prepared by adding DMPC powder to a DHPC micelle solution in deionized water that had been filtered twice through a closed-loop pumping apparatus equipped with a 0.2- μm syringe filter. Samples were prepared with final c_L values of 2.5% (w/w), with q varied from 0.17 to 2.05; and with c_L of 10% (w/w), with q varied from 0.29 to 1.72. Samples were shaken and then equilibrated for 1 h in a 40°C water bath followed by 1 h in an ice-water bath. Temperature cycling was repeated a total of three times to facilitate homogeneous mixing and produce narrow size distributions.

QLS measurements were performed at $10.0 \pm 0.1^\circ\text{C}$ ($c_L = 2.5\%$ and 10%) and 15.0°C ($c_L = 10\%$) with an Ar-ion laser (Lexel Instruments, Fremont, CA) operating at 488 nm and with a typical regulated power level of 45 mW. The time autocorrelation function of scattered light intensity at 90° was measured with a BI-9000AT digital correlator (Brookhaven Instruments, Holtsville, NY). Each 5-min QLS measurement was repeated five times.

Translational diffusion constants were derived from the decay of the correlation function, and mean hydrodynamic radii were calculated using the standard Stokes-Einstein equation for a spherical particle (Chu, 1991) and the viscosity of the solvent. The validity of this procedure was ensured by restricting the product of aggregate diameter (nm) and viscosity (cP) to less than ~ 2 . In practice this meant that bicellar size measurements at 37°C were precluded. After checking the particle sizes in samples of polystyrene beads and sodium dodecylsulfate micelles (Mazer et al., 1976), the mean radius and size distribution were determined for each bicelle solution using Cumulants, CONTIN, and NNLS algorithms (Koppel, 1972; Provencher, 1982; Morrison et al., 1985). Shape information was deduced from semilog plots of normalized scattered light intensity/ c_L versus hydrodynamic radius using analyses devised to distinguish spheres, disks, and rods in bile-salt-phospholipid mixtures (Mazer et al., 1980; Cohen et al., 1998).

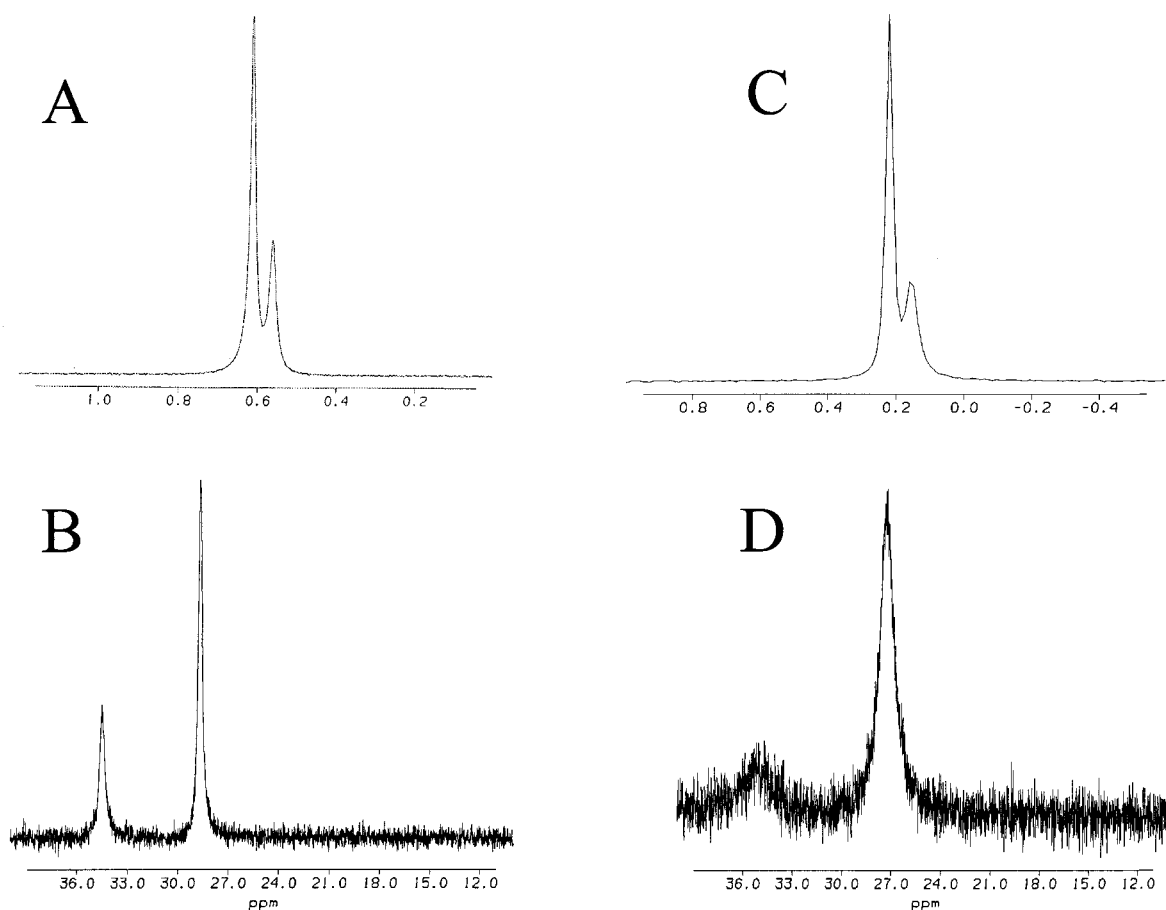


FIGURE 2 ^{31}P NMR spectra of bicelles ($q = 0.5$; $c_L = 20\%$ (w/w) or 504 mM) at 37°C (A) or 37°C (B) with 197 mM PrCl_3 or 15°C (C) or 15°C (D) with 197 mM PrCl_3 . All samples were buffered at pH 5.6 with 20 mM acetate. The spectra were recorded with a 100-ppm sweep width and referenced by placing the carrier frequency in the center of the spectrum.

Electron microscopy

DMPC/DHPC bicelle samples were prepared with $q = 0.5$ and $c_L = 20\%$ (w/w) in 10 mM 4-morpholinepropanesulfonic acid (MOPS) buffer, pH 7.0. Bicelles were then visualized in an electron microscope using a simple negative staining technique. The bicelle solution was diluted 100-fold with 10 mM MOPS (pH 7.0). A droplet of freshly diluted, unfixed bicelles was immediately applied to polylysine-treated carbon-coated grids and negatively stained with 1% uranyl acetate following the protocol of Castle and Hubbel (1976). The bicelles were placed on the copper grids immediately after the dilution (<5 min). Then, after 5 min, the grids were washed three times and stained with uranyl acetate for 1 min. The grids were dried for 30–60 min and viewed in a Zeiss EM910 electron microscope. The grids were prepared at room temperature, and the temperature during visualization remained close to room temperature. The pictures show bicelles in both dimensions and all orientations. The images is expected to be several bicelles thick based on the fact that similar images were collected under identical conditions for vesicles and other membrane structures, which are much larger than bicelles. Although it is not completely clear how the bicelle morphology is maintained during visualization, if significant time elapsed between dilution and application to the grid, no bicelles were observed. Thus, it is likely that the bicelles were kinetically trapped during visualization due to re-concentration during drying.

RESULTS AND DISCUSSION

^{31}P NMR

Fig. 2 A shows the ^{31}P NMR spectrum of a DMPC-DHPC mixture at 37°C . At 242 MHz, the separation of the DHPC and DMPC resonances was 14.52 Hz and the linewidth was ~ 5 Hz at 37°C and a q of 0.5. Only a single resonance was observed at a q of 1.0 and 35°C operating at a field strength of 109 MHz by Sanders and Schwonek (1992). This is not surprising considering that these larger bicelles tumble more slowly, resulting in broader lines as well as the fact that the experiment was carried out at lower field strength (Sanders and Schwonek, 1992). Control experiments with 2 mM DMPC and 2 mM DHPC in both chloroform and methanol yielded indistinguishable phosphorus chemical shifts for the two phospholipids (data not shown), suggesting that the two resonances observed in the DMPC-DHPC mixture arise from distinct chemical and/or magnetic environments characteristic of the aggregate structure. Because the downfield peak has an integrated area

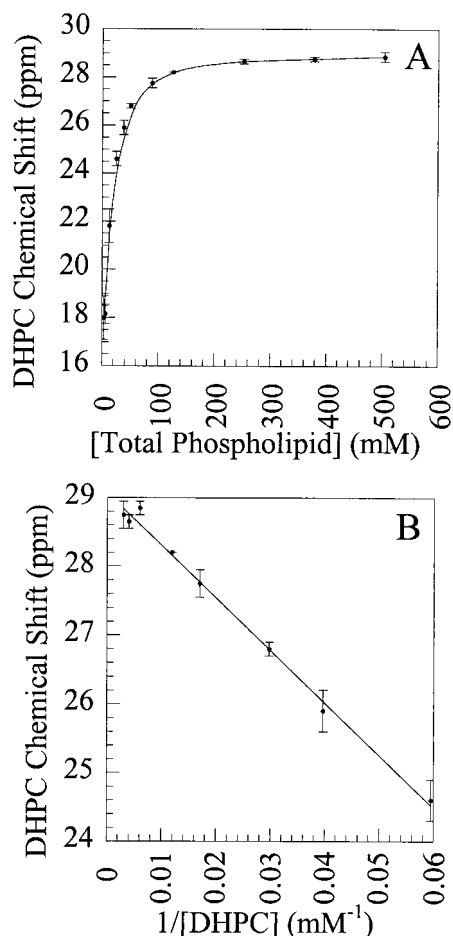


FIGURE 3 Variation of the DHPC ^{31}P chemical shift (ppm) as a function of total phospholipid concentration (mM) (A) and the inverse of the DHPC concentration (mM^{-1}) (B) at 37°C for $q = 0.5$ bicelles (slope, -78.5 ; y -intercept, 29.1 ; $R = 0.997$). The spectra were referenced by placing the carrier frequency in the center of the spectrum.

twice as large as the upfield peak and q was equal to 0.5 , it is plausible to assign the larger peak to DHPC and the smaller one to DMPC. This agreement between peak area and lipid ratio was consistent over a wide range of q (data not shown), which supports our assignment of the resonances. This interpretation also agrees with that made for headgroup proton NMR signals in dilute mixtures prepared with $q = 4$ and below the phase transition temperature of the long-chain phospholipid (Gabriel and Roberts, 1984).

To gain additional information about the ^{31}P environments, spectra were acquired in the presence of Pr^{3+} , a trivalent paramagnetic lanthanide ion. Kumar and Baumann (1991) demonstrated previously that the extent of Pr^{3+} -induced chemical shift perturbation depends upon the organization of the phospholipid: aggregated long-chain lysophospholipids shift further downfield than monomers. Similar effects were observed for both DHPC and diheptanoylphosphatidylcholine. As shown in Fig. 2 B, Pr^{3+} alters the chemical shifts of both ^{31}P resonances in $q = 0.5$

TABLE 1 Average Chemical Shifts of Lipids

| $\sim c_L$ (%) | Total lipid (mM) | DMPC (mM) | δ DMPC (ppm) | DHPC (mM) | δ DHPC (ppm) |
|----------------|------------------|-----------|---------------------|-----------|---------------------|
| 20 | 504 | 168 | 34.4 ± 0.3 | 336 | 28.8 ± 0.2 |
| 15 | 378 | 126 | 34.5 ± 0.0 | 252 | 28.6 ± 0.1 |
| 10 | 252 | 84.0 | 34.9 ± 0.0 | 168 | 28.8 ± 0.1 |
| 5 | 126 | 42.0 | 34.8 ± 0.1 | 84.0 | 28.2 ± 0.0 |
| 3.5 | 88.2 | 29.4 | 35.2 ± 0.3 | 58.8 | 27.8 ± 0.2 |
| 2 | 50.4 | 16.8 | 35.0 ± 0.0 | 33.6 | 26.8 ± 0.1 |
| 1.5 | 37.8 | 12.6 | 35.2 ± 0.1 | 25.2 | 25.9 ± 0.3 |
| 1 | 25.2 | 8.40 | 35.4 ± 0.2 | 16.8 | 24.6 ± 0.3 |
| .5 | 12.6 | 4.20 | 35.7 ± 0.1 | 8.40 | 21.8 ± 0.7 |
| 0.25 | 6.30 | 2.11 | 35.8 ± 0.3 | 4.20 | 18.0 ± 0.4 |
| 0.125 | 3.15 | 1.05 | 36.1 ± 0.1 | 2.10 | 18.2 ± 0.9 |

Shifts of lipids in bicelles ($q = 0.5$) as a function of lipid concentration (37°C , 197 mM Pr^{3+} , $20 \text{ mM acetate pH } 5.5$).

DMPC-DHPC mixtures, thus arguing against the presence of vesicular structures. The observation of a larger downfield change for DMPC is consistent with a bicellar model in which the lanthanide is chelated more effectively by DMPC in the planar region than by DHPC on the rim (Vold and Prosser, 1996). Moreover, the close correspondence of bicellar DHPC chemical shifts to micellar rather than monomer values suggests that the bicelle rim is micelle-like in its organization. Finally, ^{31}P NMR spectra acquired at 15°C (Fig. 2, C and D) and for mixtures with q values down to 0.05 (data not shown) reveal that segregation of the two phospholipid species is maintained over a wide range of experimental conditions. Although the DMPC peak is broadened noticeably at temperatures below its phase transition temperature (Fig. 2, C and D), it remains observable under all circumstances.

Fig. 3 A and Table 1 illustrate the concentration-dependent shifts of the DHPC resonance. As the total phospholipid concentration is decreased, the chemical shift of DHPC moves from micellar (28 ppm) to monomeric (18 ppm) δ DHPC values. This trend suggests that DHPC is in fast exchange between free and bicelle-associated states and that the equilibrium distribution between these forms changes progressively with lipid concentration (Ottiger and Bax, 1998; Struppe and Vold, 1998). The observed phosphorus chemical shift for DHPC in fast exchange between monomeric and bicelle-associated states may be described as

$$\delta_{\text{observed}} = X_{\text{free}}\delta_{\text{free}} + X_{\text{bicelle}}\delta_{\text{bicelle}} \quad (1)$$

where X represents mole fractions and δ represents chemical shifts. After algebraic rearrangement, Eq. 1 can be expressed in terms of the DHPC concentration:

$$\delta_{\text{observed}} = ([\text{DHPC}]_{\text{free}})([\text{DHPC}]_{\text{total}}^{-1})(\delta_{\text{free}} - \delta_{\text{bicelle}}) + \delta_{\text{bicelle}} \quad (2)$$

If the $[\text{DHPC}]_{\text{free}}$ remains constant, then a plot of δ_{observed} versus $[\text{DHPC}]_{\text{total}}^{-1}$ should yield a straight line with a y inter-

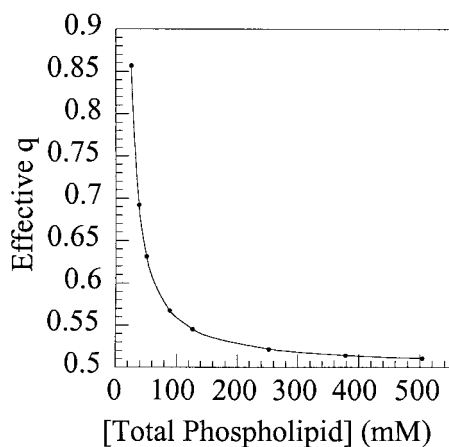


FIGURE 4 Effective bicelle q (after consideration of the free DHPC concentration) as a function of the total phospholipid concentration (mM) at 37°C. Identical results were obtained at 15°C.

cept equal to δ_{bicelle} . With this quantity in hand, and knowing that the δ_{free} is 18 ppm, the $[\text{DHPC}]_{\text{free}}$ can be calculated from the slope. Fig. 3 *B* shows that this linear relation holds for DHPC concentrations greater than 16.8 mM (corresponding to a c_L of 25.2 mM or 1% (w/w)). A straight-line fit of the data then yields $\delta_{\text{bicelle}} = 29.1$ ppm and $[\text{DHPC}]_{\text{free}} = 7$ mM. This observable concentration of free DHPC monomers agrees well with the recently published value of 4 mM, measured under slightly different experimental conditions (Ramirez et al., 2000). With $[\text{DHPC}]_{\text{free}}$ in hand, we can subtract its contribution to $[\text{DHPC}]_{\text{total}}$ and derive $q_{\text{effective}}$, the actual ratio of DMPC to DHPC in the bicelle.

Fig. 4 reveals that $q_{\text{effective}}$ remains essentially constant at 0.5 if $c_L \geq 130$ mM (5% (w/w)). Below that concentration, $q_{\text{effective}}$ increases significantly as c_L decreases. According to ideal bicelle theory (Vold and Prosser, 1996), the increase in $q_{\text{effective}}$ should be accompanied by an increase in bicelle size as the planar region is enlarged. Qualitatively similar variations in size have also been observed for phospholipid-bile salt mixtures (Mazer et al., 1980; Stark and Roberts, 1984); overall dilution enhances the proportion of the bile-salt detergent that exists in free form to maintain the intermicellar concentration, and results in the formation of a larger detergent-poor mixed-lipid aggregate.

The modest downfield shift of the DMPC resonance that occurs as c_L is decreased (Table 1) indicates an increase in the number of Pr^{3+} ions associated with this phospholipid, which would be expected if the planar region of the bicelle increased in size. Because the observed chemical shift of DMPC may be viewed as a weighted average from two environments, those molecules that are secluded in the bicelle center and those that are closer to the DHPC on the rim, the downfield shift may be interpreted as an increase in the proportion of DMPC molecules within the central bilayer region due to an increase in bicelle size.

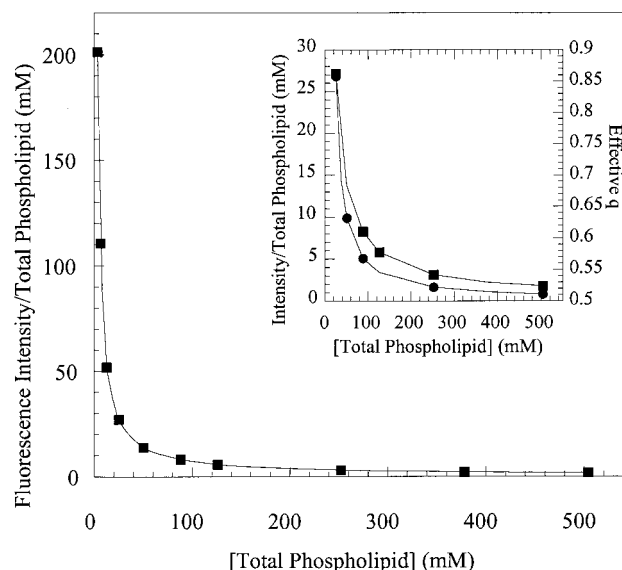


FIGURE 5 Total fluorescence intensity of 5 μM ANTS (normalized for changes in lipid concentration) in bicelles ($q = 0.5$) as a function of total phospholipid concentration (mM) at 37°C. The inset shows an enlarged region for $c_L > 25$ mM to highlight the similarity between the increase in ANTS fluorescence and the increase in effective q between 25 M and 130 mM total lipid shown in Fig. 4.

Fluorescence spectroscopy

To further probe the issue of increasing bicelle size in the concentration range of 25–130 mM, fluorescence experiments were performed using ANTS. This water-soluble fluorophore does not partition significantly into hydrophobic environments (Kuwahara and Verkman, 1988; Ye and Verkman, 1989). In a bicellar solution, there are three major environments into which the ANTS fluorophore could partition: 1) bulk water, 2) interfacial water of the planar region, and 3) interfacial water associated with the bicelle rim. Although the fluorescence emission wavelength of ANTS is virtually insensitive to the polarity of its environment, its emission intensity does reflect polarity. It is expected that the emission intensity will be highest for ANTS in the interfacial water of the bicelle planar region (least polar environment due to phospholipid packing), followed by the bicelle rim (less compact phospholipid packing), and finally, by bulk water. Moreover, the observed fluorescence emission spectrum for ANTS in a bicellar solution could contain contributions from each of these three environments.

The total fluorescence intensity per phospholipid increases dramatically as c_L decreases (Fig. 5). This increase is explained most readily by a growth in aggregate size. Although the total bicelle surface area remains constant with changing q , the relative contributions of the rim and the planar region to the total surface area do change (Vold and Prosser, 1996). As bicelle size increases, the planar region

accounts for a larger percentage of the total surface area into which the ANTS can partition and results in the observed increase in total fluorescence intensity. As shown in the inset of Fig. 5, this trend correlates nicely with the increase in $q_{\text{effective}}$ for $25 \text{ mM} < c_L < 130 \text{ mM}$ derived from the ^{31}P NMR data (Fig. 4).

An interesting phenomenon occurs as the total DHPC concentration approaches and dips below 7 mM ($c_L = 25.2 \text{ mM}$). In this range, the DHPC chemical shift becomes close to that of DHPC monomers, indicating that the overwhelming majority of DHPC molecules are no longer bicelle-associated (Table 1). If all of the DHPC were free, one would expect the insoluble DMPC to precipitate out of solution, but this is not observed. To examine the situation further, two separate solubilization experiments were performed under the same conditions used to prepare bicelle samples (room temperature). If a sufficient portion of 2.10 mM DHPC monomers was added to 1.05 mM DMPC multilamellar vesicles (MLVs) to achieve a q of 0.5, the resulting dispersion remained cloudy and never dissolved. Using this preparation method, the DHPC was unable to solubilize the DMPC. However, if a portion of 250 mM DHPC micelles was added to 1.05 mM DMPC MLVs, the solution immediately clarified and remained clear indefinitely after dilution to a final concentration of 2.10 mM DHPC. This phenomenon seems to be unique to mixtures of lipids with low q . Our hypothesis is that micellar DHPC can solubilize DMPC MLVs, but that upon dilution, the DHPC reverts to monomers and leaves behind DMPC vesicles. There is precedent for such vesicle formation in a system of egg PC solubilized by the bile salt taurocholate (Stark et al., 1985). A similar phenomenon has also been reported in conjunction with the preparation of vesicles using the alcohol injection method (Kensil and Dennis, 1985; Kremer and Wiersema, 1977). In the DMPC-DHPC system, support for such a dramatic change in aggregate morphology comes from the observation of a significant increase in normalized ANTS fluorescence intensity at low phospholipid concentrations (Fig. 5).

Dynamic light scattering

Fig. 6 illustrates the smooth dependence of mean hydrodynamic radius on the DMPC:DHPC ratio and the narrow size distribution characteristic of our δ -isotropic bicelle solutions. As the proportion of long-chain phospholipid is increased, the hydrodynamic radii of the aggregates increase from 3 to 6 nm when $c_L = 10\%$ (Fig. 6) and from 4 to 10 nm when $c_L = 2.5\%$ (data not shown). As reported previously in bile salt-lecithin mixed micelles and noted earlier, the aggregates are expected to grow in more dilute solutions, presumably because a greater proportion of the available DHPC is drawn out of the bicellar particles to maintain the interaggregate concentration (Mazer et al., 1980; Cohen et al., 1998). For a given value of q , the observation of larger

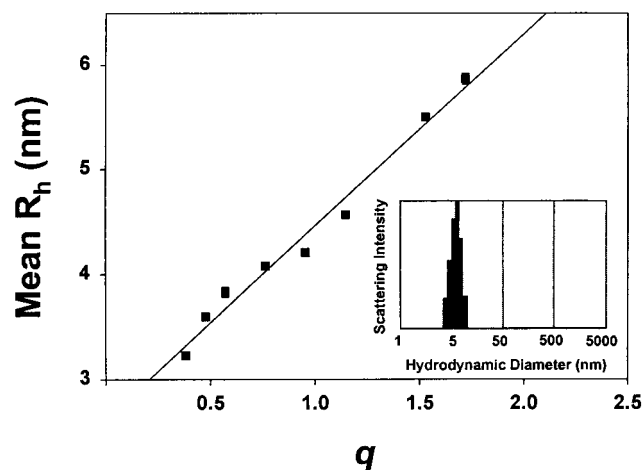


FIGURE 6 Effect of phospholipid ratio (q) on the mean hydrodynamic radii (R_h) of aggregates formed in solutions with a total lipid concentration (c_L) of 10% (w/w) and temperature of 10°C ; a similar trend is found for $c_L = 2.5\%$ (w/w). Error bars represent typical standard deviations of five measurements on the same lipid sample. The inset shows the monodisperse aggregate size distribution determined by the CONTIN method for a bicellar solution with $q = 0.376$ and $c_L = 2.5\%$ (w/w).

bicelles at $c_L = 2.5\%$ follows the trend deduced above from ^{31}P NMR and supported by the fluorescence studies. In the following analysis, the value of q and not q_{eff} is used so as to be consistent with previously derived equations. It is important to note that even at a low c_L of 2.5% (w/w), a q of 0.5 corresponds to a q_{eff} of 0.63, which has a negligible effect on the results obtained.

To deduce the aggregate shape, four models were tested using the formalism of Mazer and co-workers (1980), as augmented by Cohen et al. (1998). Fig. 7 shows a semilog plot of the scattered light intensity divided by total lipid concentration (and normalized to the minimum value of this ratio) as a function of the mean hydrodynamic radius (R_h). The experimental dependence, obtained by varying q between 0.3 and 1.7, was compared with theoretical curves for spheres, disks, stiff rods, and flexible (worm-like) rods. Excellent agreement was found between the experimental data and a disk-like model for the DMPC-DHPC bicellar aggregates. In these calculations, the diameter of the rod or the thickness of the disk were taken as 5.0 nm, reflecting the length of extended phospholipid acyl chains in a bilayer arrangement (Small, 1967) plus a 1.0-nm water layer that diffuses along with the aggregates (Cantor and Schimmel, 1980). The 5.0-nm dimension corresponds with previous NMR relaxation-based estimates of disk thickness in DMPC-detergent micelles (Sanders et al., 1994), and the presence of such a water layer is also supported by solid-state deuterium NMR studies of D_2O in the presence of oriented bicelles (Losonczi and Prestegard, 1998a). The commonly used value of 4.0 nm led to identical conclusions with regard to aggregate shape. The analysis of aggregate

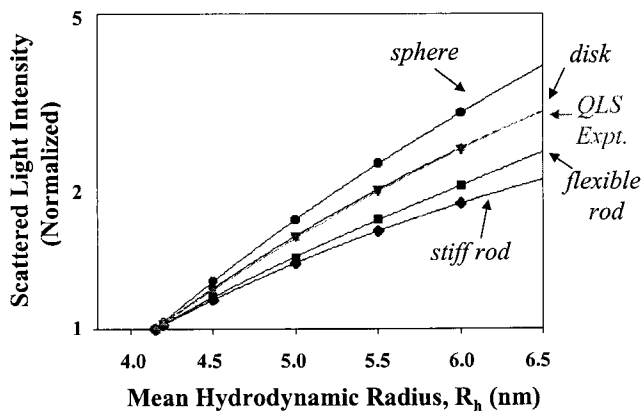


FIGURE 7 Variation of normalized scattered light intensity $((I/C)/(I/C)_{\min})$ with mean hydrodynamic radius (R_h) for mixed phospholipid aggregates of different shapes. A scattering angle of 90° and aggregate size (rod or sphere diameter, disk thickness) of 5.0 nm were used in the calculations. The curves correspond to spheres (●), disks (▼), stiff rods (◆), flexible rods (■), and experimental data for $c_L = 10\%$ (w/w) (gray triangles). Similar results were obtained for $c_L = 2.5\%$ (w/w); in both cases the measured hydrodynamic radii were determined by the method of cumulants (Koppel, 1972).

shape was restricted to q values for which the particle size was narrowly defined, ensuring that the scattered light intensity and lipid concentrations were attributable solely to bicellar aggregates of uniform size. Possible contributions to the scattered light intensity from interaggregate interactions (Phillies, 1990) were ruled out by the linear relationship observed between the power of the incident light and the number of scattered photons per unit time (data not shown).

With this shape information in hand, it was possible to compare the hydrodynamic radii (R_h) measured by QLS methods with the predictions made for ideal bicelles (Vold and Prosser, 1996). First, using a disk thickness (t) of 5.0 nm, the value of the disk radius (r') was found from the experimental hydrodynamic radii (R_h) at various DMPC/DHPC ratios using the following relation (Mazer et al., 1980):

$$R_h = \frac{3}{2} r' \left\{ \left[1 + \left(\frac{t}{2r'} \right)^2 \right]^{1/2} + \frac{2r'}{t} \ln \left[\frac{t}{2r'} + \left[1 + \left(\frac{t}{2r'} \right)^2 \right]^{1/2} \right] - \frac{t}{2r'} \right\}^{-1} \quad (3)$$

The values of r' obtained were plotted against q (Fig. 8, Δ). To ascertain whether the bicelles were behaving according to the ideal bicelle model, the disk radius, r' , was related to the ideal bicelle quantity ($R + r$) where R is the radius of the planar region and r is the radius of the rim (Vold and Prosser, 1996) (cf. Fig. 1 B). Then, taking r from independent measurements on DHPC micelles ($r = 2$ nm (Eum et al., 1989; Vold and Prosser, 1996)), Eq. 4 was used to

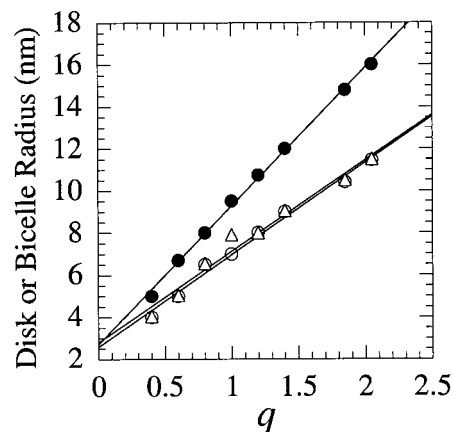


FIGURE 8 Influence of the phospholipid ratio (q) on the disk radius (r') and sum of bicelle radii ($R + r$), as determined from QLS measurements with $c_L = 2.5\%$ (w/w) (Δ), an ideal bicelle theoretical model (●), and a refined bicelle model (○).

calculate R so that the quantity ($R + r$), which relates directly to the calculated values of r' , could be obtained.

$$R = \frac{1}{2} r q [\pi + (\pi^2 + 8/q)^{1/2}] \quad (4)$$

As shown in Fig. 8, a plot of ($R + r$) versus q reveals similar general trends but a quantitative disparity between the dynamic light scattering data (Δ) and this ideal bicelle model (●).

The disparity between the data and the ideal bicelle model was thought to be due to the assumption in the ideal bicelle model that the DMPC and DHPC have a common headgroup area. Therefore, the ideal bicelle theory was refined based on the likely greater surface area occupied by lipid molecules at the curved bicelle rim (DHPC) as compared with the central planar domain (DMPC). With this modification we obtained

$$R = \frac{1}{2} k r q [\pi + (\pi^2 + 8k/q)^{1/2}] \quad (5)$$

where k is the ratio of headgroup areas for DHPC as compared with DMPC. The parameter k is available experimentally, because values of the headgroup areas have been estimated as 1.0 nm² for DHPC micelles (Gabriel and Roberts, 1987) and 0.6 nm² for DMPC multibilayers (Koenig et al., 1997). Using these data, excellent agreement was obtained between the refined bicelle theory (Fig. 8, ○) and the dynamic light scattering data (Fig. 8, Δ).

Electron microscopy

Fig. 9 shows an electron micrograph of a $q = 0.5$ and $c_L = 20\%$ DMPC/DHPC mixture. The image presents the aggregates in all possible orientations with respect to the grid because the sample is several bicelles thick. The shape of the aggregates appears either circular or oblong, and mea-

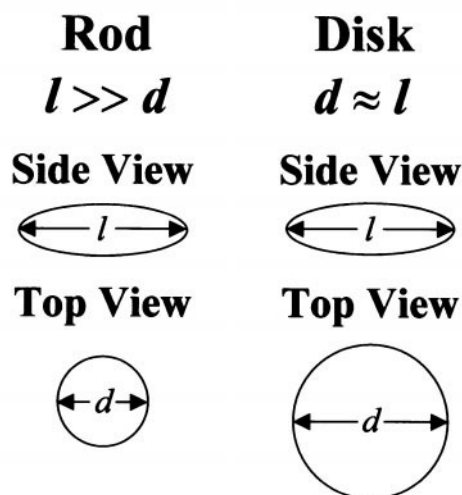
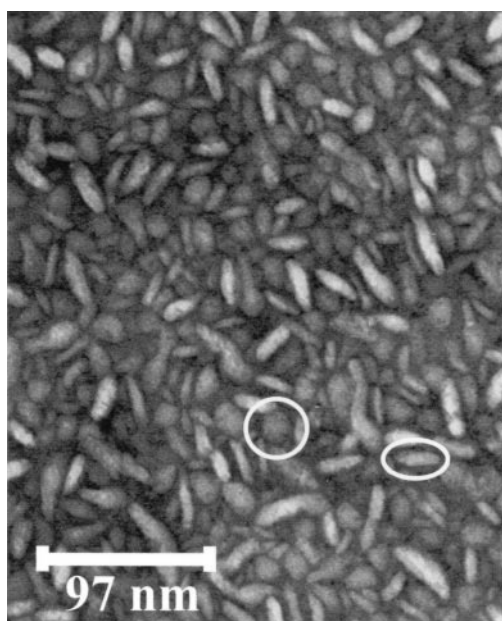


FIGURE 9 Electron micrograph of a $q = 0.5$ DMPC/DHPC mixture obtained after 100-fold dilution (room temperature) of a 20% (w/w) solution (504 mM; 10 mM, pH 7.0 MOPS). Samples were immediately transferred to the grid for negative staining (Castle and Hubbell, 1976). The picture was obtained at $\times 100,000$ magnification and expanded by a factor of 2.75 from the original film. Calibration grids indicated a $\pm 5\%$ correction to the nominal dimensions. Schematic diagrams of possible aggregate shapes are shown below for comparison.

measurements taken of those bicelles in the topmost layer gives a diameter (circular view) and length (oblong view) of 21 ± 2 nm and 26 ± 2 nm, respectively. Because the lengths (oblong view) are very close to the diameters (circular view), the aggregate shape is consistent only with a disk-shaped model (Fig. 9, $d \approx l$). Rods, on the other hand, would have a greater length than diameter (Fig. 9, $l \gg d$). The measured disk thickness t is $\sim 5 \pm 1$ nm, in accord with the thickness expected for a DMPC bilayer. However, the

bicelle diameter is larger than predicted by the ideal bicelle theory. This suggests that the electron micrograph captured the bicelles in a kinetically trapped state where they were increasing in size due to the extreme sample dilution that took place before deposition of the sample on the grid. Because the sample was transferred quickly to the grid, the bicelle structure was likely maintained because the sample reconcentrated upon drying. This is corroborated by further results that demonstrated that the discoidal shape was not present when an electron micrograph of the same diluted sample was obtained the next day.

CONCLUSIONS

Using several complementary physical techniques, we have demonstrated that mixtures of DMPC and DHPC at a $q = 0.5$ exhibit the phospholipid domain structure and discoidal shape predicted in bicellar models (Vold and Prosser, 1996) and established experimentally for preparations with $q > 2$ (Sanders et al., 1994; Vold and Prosser, 1996). ^{31}P NMR supports the hypothesis that the two lipids are segregated in different aggregation states within the bicelle, a regular bilayer of long-chain DMPC and a curved rim of short-chain DHPC. Moreover, the bicellar DHPC is in fast exchange with a significant (7 mM) concentration of DHPC monomers that remains constant over a wide range of lipid concentrations. As the total lipid concentration drops, a significant increase in aggregate size is evidenced from measurements of ^{31}P chemical shifts, ANTS fluorescence intensity, and quasielastic light scattering. Dynamic light scattering and electron microscopy reveal that mixtures of $q = 0.5$ bicelles are composed of discoidal aggregates that have dimensions that agree with theoretical predictions (Vold and Prosser, 1996). Taken together, these experiments show that $q = 0.5$ bicelles contain a true bilayer and serve as useful mimetic membranes for solution-state studies of peptides and proteins.

We thank Dr. Yitzhak Tor (UCSD) and Dr. Kerry K. Karukstis (Harvey Mudd College, Claremont, CA) for use of their fluorimeters, Dr. John Wright (UCSD) for help with the NMR experiments, and Stephanie R. Lloyd for technical assistance with the electron microscopy.

This work was supported by National Institutes of Health (5 R01 GM54034) and National Science Foundation (CHE9632618) grants to R.R.V. and by GM20501 (supporting R.A.D.). J.A.W. was supported by a La Jolla Interfaces in Science predoctoral fellowship from the Burroughs Wellcome Fund, and K.J.G. was supported by an National Institutes of Health Heme and Blood Proteins Training grant. R.E.S. acknowledges support from the New York State Higher Education Applied Technology Program and the CUNY Center for Applied Biomedicine and Biotechnology.

REFERENCES

- Cantor, C. R., and P. R. Schimmel. 1980. *Biophysical Chemistry*. W. H. Freeman and Co., San Francisco.

- Castle, J. D., and W. L. Hubbell. 1976. Estimation of membrane surface potential and charge density from the phase equilibrium of a paramagnetic amphiphile. *Biochemistry*. 15:4818–4831.
- Chu, B. 1991. *Laser Light Scattering: Basic Principles and Practice*. Academic Press, New York.
- Cohen, D. E., G. M. Thurston, R. A. Chamberlin, G. B. Benedek, and M. C. Carey. 1998. Laser light scattering evidence for a common wormlike growth structure of mixed micelles in bile salt- and straight-chain detergent-phosphatidylcholine aqueous systems: relevance to the micellar structure of bile. *Biochemistry*. 37:14798–14814.
- Eum, K. M., G. Riedy, K. H. Langley, and M. F. Roberts. 1989. Temperature-induced fusion of small unilamellar vesicles formed from saturated long-chain lecithins and diheptanoylphosphatidylcholine. *Biochemistry*. 28:8206–8213.
- Gabriel, N. E., and M. F. Roberts. 1984. Spontaneous formation of stable unilamellar vesicles. *Biochemistry*. 23:4011–4015.
- Gabriel, N. E., and M. F. Roberts. 1987. Short-chain lecithin/long-chain phospholipid unilamellar vesicles: asymmetry, dynamics, and enzymatic hydrolysis of the short-chain component. *Biochemistry*. 26:2432–2440.
- Howard, K. P., and S. J. Opella. 1996. High resolution solid-state NMR spectra of integral membrane proteins reconstituted into magnetically oriented phospholipid bilayers. *J. Magn. Reson.* 112:91–94.
- Kensil, C. R., and E. A. Dennis. 1985. Action of cobra venom phospholipase A₂ on large unilamellar vesicles: comparison with small unilamellar vesicles and multibilayers. *Lipids*. 20:80–83.
- Koenig, B. W., H. H. Strey, and K. Gawrisch. 1997. Membrane lateral compressibility determined by NMR and x-ray diffraction: effect of acyl chain polyunsaturation. *Biophys. J.* 73:1954–1966.
- Koppel, D. E. 1972. Analysis of macromolecular polydispersity in intensity correlation spectroscopy: the method of cumulants. *J. Chem. Phys.* 57:4814–4820.
- Kremer, J. M., and P. H. Wiersema. 1977. Exchange and aggregation in dispersions of dimyristoyl phosphatidylcholine vesicles containing myristic acid. *Biochim. Biophys. Acta.* 471:348–360.
- Kumar, V. V., and W. J. Baumann. 1991. Lanthanide-induced phosphorus-31 NMR downfield chemical shifts of lysophosphatidylcholines are sensitive to lysophospholipid critical micelle concentration. *Biophys. J.* 59:103–107.
- Kuwahara, M., and A. S. Verkman. 1988. Direct fluorescence measurement of diffusional water permeability in the vasopressin-sensitive kidney collecting tubule. *Biophys. J.* 54:587–593.
- Losonczi, J. A., and J. H. Prestegard. 1998a. Improved dilute bicelle solutions for high-resolution NMR of biological macromolecules. *J. Biomol. NMR.* 12:447–451.
- Losonczi, J. A., and J. H. Prestegard. 1998b. Nuclear magnetic resonance characterization of the myristoylated, N-terminal fragment of ADP-ribosylation factor 1 in a magnetically oriented membrane array. *Biochemistry*. 37:706–716.
- Mazer, N. A., G. B. Benedek, and M. C. Carey. 1976. An investigation of the micellar phase of sodium dodecylsulfate in aqueous sodium chloride solution using quasielastic light scattering spectroscopy. *J. Phys. Chem.* 80:1075–1085.
- Mazer, N. A., G. B. Benedek, and M. C. Carey. 1980. Quasielastic light-scattering studies of aqueous binary lipid systems: mixed micelle formation in bile salt-lecithin solutions. *Biochemistry*. 19:601–615.
- Morrison, I. D., E. F. Grabowski, and C. A. Herb. 1985. Improved techniques for particle size determination by QELS. *Langmuir*. 1:496–501.
- Ottiger, M., and A. Bax. 1998. Characterization of magnetically oriented phospholipid micelles for measurement of dipolar couplings in macromolecules. *J. Biomol. NMR.* 12:361–372.
- Phillies, G. D. J. 1990. Quasielastic light scattering. *Anal. Chem.* 62:1049A–1057A.
- Provencher, S. W. 1982. A constrained regularization method for inverting data represented by linear algebraic or integral equations. *Comput. Phys. Commun.* 27:213–228.
- Ram, P., and J. H. Prestegard. 1988. Magnetic field induced ordering of bile salt/phospholipid micelles: new media for NMR structural investigations. *Biochim. Biophys. Acta.* 940:289–294.
- Ramirez, B. E., O. N. Voloshin, R. D. Camerini-Otero, and A. Bax. 2000. Solution structure of DinI provides insight into its mode of RecA inactivation. *Protein Sci.* 9:2161–2169.
- Sanders, C. R., B. J. Hare, K. P. Howard, and J. H. Prestegard. 1994. Magnetically oriented phospholipid micelles as a tool for the study of membrane associated molecules. *Prog. NMR Spectrosc.* 26:421–444.
- Sanders, C. R., and G. C. Landis. 1995. Reconstitution of membrane proteins into lipid-rich bilayered mixed micelles for NMR Studies. *Biochemistry*. 34:4030–4040.
- Sanders, C. R., and J. H. Prestegard. 1990. Magnetically orientable phospholipid bilayers containing small amounts of a bile salt analogue, CHAPSO. *Biophys. J.* 58:447–460.
- Sanders, C. R., J. E. Schaff, and J. H. Prestegard. 1993. Orientational behavior of phosphatidylcholine bilayers in the presence of aromatic amphiphiles and a magnetic field. *Biophys. J.* 64:1069–1080.
- Sanders, C. R., and J. P. Schwonek. 1992. Characterization of magnetically orientable bilayers in mixtures of dihexanoylphosphatidylcholine and dimyristoylphosphatidylcholine by solid-state NMR. *Biochemistry*. 31:8898–8905.
- Small, D. M. 1967. Phase equilibria and structure of dry and hydrated egg lecithin. *J. Lipid Res.* 8:551–557.
- Stark, R. E., G. J. Gosselin, J. M. Donovan, M. C. Carey, and M. F. Roberts. 1985. Influence of dilution on the physical state of model bile systems: NMR and quasi-elastic light scattering investigations. *Biochemistry*. 24:5599–5605.
- Stark, R. E., and M. F. Roberts. 1984. 500 MHz ¹H NMR studies of bile salt-phosphatidylcholine mixed micelles and vesicles: evidence for differential motional restraint on bile salt and phosphatidylcholine resonances. *Biochim. Biophys. Acta.* 770:115–121.
- Struppe, J. O., E. A. Komives, S. S. Taylor, and R. R. Vold. 1998. ²H NMR studies of a myristoylated peptide in neutral and acidic phospholipid bicelles. *Biochemistry*. 37:15523–15527.
- Struppe, J. O., and R. R. Vold. 1998. Dilute bicellar solutions for structural NMR work. *J. Magn. Reson.* 135:541–546.
- Struppe, J. O., J. A. Whiles, and R. R. Vold. 2000. Acidic phospholipid bicelles: a versatile model membrane system. *Biophys. J.* 78:281–289.
- Tjandra, N., and A. Bax. 1997. Direct measurements of distances and angles in biomolecules by NMR in a dilute liquid crystalline medium. *Science*. 278:1111–1113.
- Vold, R. R., and R. S. Prosser. 1996. Magnetically oriented phospholipid bilayered micelles for structural studies of polypeptides. Does the ideal bicelle exist? *J. Magn. Reson. B.* 113:267–271.
- Vold, R. R., R. S. Prosser, and A. J. Deese. 1997. Isotropic solutions of phospholipid bicelles: a new membrane mimetic for high-resolution NMR studies of polypeptides. *J. Biomol. NMR.* 9:329–335.
- Whiles, J. A., R. Brasseur, K. J. Glover, G. Melacini, E. A. Komives, and R. R. Vold. 2001. The orientation and effects of mastoparan X on phospholipid bicelles. *Biophys. J.* 80:280–293.
- Ye, R., and A. S. Verkman. 1989. Simultaneous optical measurement of osmotic and diffusional water permeability in cells and liposomes. *Biochemistry*. 28:824–829.